J Membrane Biol (2012) 245:97–105
DOI 10.1007/s00232-012-9418-6

Hyperpolarization of the Membrane Potential in Cardiomyocyte Tissue Slices by the Synchronization Modulation Electric Field

Robin Dando · Zhihui Fang · Wei Chen

Received: 20 June 2011 / Accepted: 31 January 2012 / Published online: 23 February 2012

Abstract Our previous studies have shown that a specially designed, so-called synchronization modulation electric field can entrain active transporter Na/K pumps in the cell membrane. This approach was previously developed in a study of single cells using a voltage clamp to monitor the pump currents. We are now expanding our study from isolated single cells to aggregated cells in a 3-dimensional cell matrix, through the use of a tissue slice from the rat heart. The slice is about 150 μm in thickness, meaning the slices contain many cell layers, resulting in a simplified 3-dimensional system. A fluorescent probe was used to identify the membrane potential and the ionic concentration gradients across the cell membrane. In spite of intrinsic cell-to-cell interactions and the difficulty in stimulating cell aggregation in the tissue slice, the oscillating electric field increased the intracellular fluorescent intensity, indicating elevation of the cell ionic concentration and hyperpolarization of the cell membrane. Blockage of these changes by ouabain confirmed that the results are directly related to Na/K pumps. These results along with the backward modulation indicate that the synchronization modulation electric field can influence the Na/K pumps in tissue cells of a 3-dimensional matrix and therefore hyperpolarize the cell membrane.

Keywords Cardiac tissue slice · Hyperpolarization · Synchronization · Modulation · Na/K pump

R. Dando · Z. Fang · W. Chen (✉)
Cellular and Molecular Biophysics Lab, Department of Physics, University of South Florida, 4202 E. Fowler Ave., Tampa, FL 33620, USA
e-mail: wchen@cas.usf.edu

Introduction

The electrogenic action of the Na/K-ATPase or Na/K pump has been thoroughly documented since its initial characterization around 50 years ago (Skou 1957; Post and Jolly 1957; Albers 1967). The pump molecule, in each pumping cycle, extrudes 3 Na ions and pumps in 2 K ions against their electrochemical potential barriers by consuming metabolic energy from hydrolysis of one ATP molecule. The major function of the Na/K pump is to maintain the intracellular ionic concentration and the potential difference across the cell membrane. The ionic concentration gradient and the membrane potential play a significant role in many cell functions.

Many diseases and disorders are associated with dysfunction of Na/K pumps due to either lack of metabolic energy to fuel the pump molecules, a defect in the mechanism to control the pumps or deficiency of the pump contents. Heart failure often involves a shortage of blood and oxygen, which may result in a deficiency of ATP molecules (Conway et al. 1974). Membrane electroporation in lightning and electric shock will result in loss of ionic concentration gradients (Lee and Kolodncy 1987; Lee et al. 1988). Without quick reinstatement of the ionic concentration gradient, cell excitability may be lost and cells may swell and undergo necrosis. Diminished Na/K pump activity has been observed in several tissues prone to diabetic complications, including peripheral nerves (Stevens et al. 1993; Sima et al. 2004), blood vessels (Wahren et al. 2000), skeletal and cardiac muscles (Yuk-Chow et al. 1993), retinal cells (Phipps et al. 2006) and kidney renal tubules (Scherzer et al. 2000). In addition, in many diseases, Na/K pump functions are impaired by a significant deficiency in the pump itself, such as Alzheimer disease (Evertsen et al. 1997), Huntington disease (Everts et al. 1990), myotonic

dystrophy (Desnuelle et al. 1982), phosphorylase deficiency (De Paoli et al. 2002) and McArdle disease (Haller et al. 1998). How to activate the pump functions is an important scientific question relevant to disease treatment and emergency management.

Significant efforts have been made in the past to electrically modulate the pump function. Many investigators have focused on the interaction of the oscillating electric field resonance with the pump's intrinsic oscillating frequency, where the intrinsic frequencies are assumed to exist (Teissie and Tsong 1980; Serpersu and Tsong 1983; Tsong and Astumian 1987; Blank and Soo 1989; Xie et al. 1994). Several theoretical models have been developed, including a thermal noise model of weak electric field–induced pump activation (Weaver and Astumian 1990), a brownian motion model (Astumian 1997; Tsong 2002) and an adiabatic pump model (Astumian 2003).

Recently, a practical technique was developed by our group to effectively control the pump function. Theoretical analysis of the synchronization modulation (Chen 2008), computer simulation (Chen and Huang 2008; Huang et al. 2009) and experimental results (Chen et al. 2007, 2008) have been reported previously. Here, we only briefly describe the underlying mechanisms involved in the technique and the technique protocol. The technique was developed by introducing the concept from an electronic synchrotron accelerator to the biological system. The technique consists of two steps: first, a specially designed pulsed oscillating electric field is applied to force or synchronize the individual pump molecules to run at the same pace as the field oscillation so that the Na transport from individual pumps is entrapped into the positive half-cycle, while all the K transporters are similarly entrapped in the negative half-cycle; second, the field frequency is gradually changed, either increased or decreased following a step-change pattern. By carefully maintaining the pump synchronization, the pump molecules can be entrained and either accelerated or decelerated, to a defined pumping rate (Chen et al. 2007, 2008).

Our whole-cell patch-clamp experiments on single skeletal muscle cells have demonstrated effective synchronization of the Na/K pumps and realized significant acceleration of the pumping rate up to 10-fold (Chen et al. 2007, 2008). We also showed that the oscillating electric field can elevate or hyperpolarize the membrane resting potential of single intact skeletal muscle fibers (Chen and Dando 2007, 2008).

When single cells are organized into tissues, these natural cell aggregations have resultant electrical properties through tissue matrix structure, cell-to-cell interactions and regulatory mechanisms associated with specific physiological functions. In addition, the cell aggregations with narrow intercellular spaces may obstruct the pathway of the field application to generate an oscillating membrane potential across each individual cell membrane. Our postulation is that the oscillating electric field should be able to penetrate the tissue through the interstitial fluid between the cells, alternating the membrane potential and hence activating the Na/K pumps in inner-layer cells. Because of active entrainment of the pump molecules, the technique should be able to increase the cell ionic concentration gradients and hyperpolarize the membrane potential in tissues.

Here, we report our experimental results in application of the synchronization modulation electric field to cardiomyocytes in tissue slices. Mammalian cardiomyocytes contain some of the highest expression of Na/K-ATPase outside of the CNS. The sliced tissue is estimated to be around five to eight cells thick. Confocal microscopic imaging with slow fluorescent probes was used to monitor the field-induced potential changes. The study demonstrated that the synchronization modulation electric field can effectively hyperpolarize the cell membrane beyond the normal resting potential by activating the Na/K pumps in tissue cells.

Methods

All animal work was carried out under full Institutional Animal Care and Use Committee approval. Adult male Sprague–Dawley rats weighing 200–300 g were anesthetized using 100 mg/kg thiobutabarbitol (Inactin; Sigma-Aldrich, St. Louis, MO), injected intraperitoneally; and the hearts were quickly dissected from the pericardium and placed in cooled phosphate-buffered saline (PBS) solution, oxygenated with 95% oxygen, 5% CO_2. The fat, arteries and aorta were removed in solution; and the atria were dissected away. Dissected tissue from the left ventricle was briefly dried and brought into contact with the stage of an Electron Microscopy Sciences OTS 4500 oscillating tissue slicer (Warner Instruments, Hamden, CT), which was previously coated with industrial adhesive. Fifteen seconds was deemed sufficient to assure adequate adhesion, with the tissue subsequently resubmerged in oxygenated PBS, this time in the slicer bath. For our application, slices of 150 μm were deemed to be adequate, allowing a thin enough slice for the application but ensuring that the slice was still thick enough to approximate a 3-dimensional region of tissue.

Slices were then placed in a custom-made experimental chamber (a modified Ussing chamber) filled with cell culture solution. A schematic of the chamber is displayed in Fig. 1, with a transparent base to allow fluorescence to pass, with a small working distance from the microscope objective. The slice was sealed airtight (around 1 MΩ

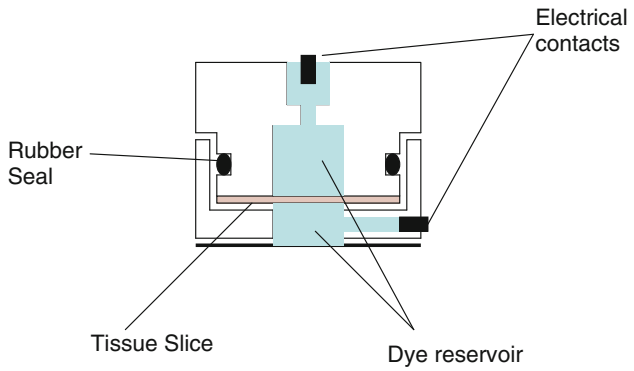

Fig. 1 Modified Ussing chamber, with slice surrounded by two dye reservoirs and electrical contacts made to *top* and *bottom*

sealing resistance) into two compartments, the top and bottom, ensuring the voltage drop of the electric field applied to the two compartments was mainly across the tissue slice. Electrical contacts were made with agar bridges to two compartments in order to minimize junction potential. Adequate dye reservoirs were maintained on either side of the tissue slice, to provide enough dye molecules for the cells, while still being small enough to not interfere with the microscope depth of field.

Membrane potential was measured using fluorescence probe tetramethylrhodamine ethyl ester (TMRE). Fluorescence images were taken using standard rhodamine optics, employing 488 nm argon laser excitation and 505 nm long pass emission filter and a fully computer-controlled Olympus (Center Valley, PA) IX81 confocal microscope system, running the Fluoview Tiempo (Olympus, Tokyo, Japan) analysis package. The confocal microscope is able to focus on a specific cell layer inside the tissue in order to accurately and efficiently monitor the field-induced fluorescence-intensity changes inside the tissue. A 10× dry objective and a confocal aperture of 80 nm was used in each of these readings.

Potentiometric dye, TMRE, was selected due to its superior potential sensitivity. TMRE dye belongs to a class known as Nernstian dyes, initially developed by Waggoner (1976). In contrast to many other fluorescent dyes that exhibit fluorescence only when binding with specific molecules, TMRE always fluoresces. The lipophilicity of TMRE, combined with the delocalization of the positive charge on the dye molecules, renders them membrane-permeant (Tsien and Waggoner 1990; Loew 1993). The high membrane permeability and the positive charge allow the TMRE molecules to easily penetrate the membrane into the cells due to the negative intracellular membrane potential. When reaching equilibrium, the ratio of the intracellular dye molecules, and hence fluorescence intensity, over those on the extracellular side is governed by the membrane potential difference. Whenever the membrane potential changes, the TMRE molecules redistribute themselves, crossing the membrane and exhibiting a different fluorescent intensity ratio.

It takes time for TMRE molecule redistribution. Therefore, TMRE is called a "slow dye," which fit our purpose well because we were not interested in the oscillating membrane potential induced by the applied electric field. Instead, we were interested in the DC shift, especially the hyperpolarization, of the membrane potential, which is a result of ionic concentration changes due to continuous activation of the Na/K pumps.

TMRE fluorescence probe and confocal microscope imaging have long been used to study membrane potential changes in our lab (Chen and Dando 2007, 2008). In this article, no attempt is made to measure the absolute value of the membrane potential. Instead, we demonstrate the capability of the oscillating electric field to hyperpolarize the membrane potential of a 3-dimensional cellular aggregation in a superfused tissue slice.

Solutions used were as follows (in mM), with chemicals obtained from Sigma unless otherwise noted: Krebs HEPES (KH) solution, 118 NaCl, 10 HEPES, 4.7 KCl, 1.5 $CaCl_2$, 1.1 $MgSO_4$, 1.2 KH_2PO_4, 5.6 glucose; experimental solution, same as KH solution with 1 μM TMRE, 1 μM TTX; culture medium, DMEM with 15% FBS and 1% penicillin/streptomycin. All solutions were titrated to pH 7.4 at 25°C.

Stimulation was provided through a purpose-designed LabVIEW program (Texas Instruments, Dallas, TX), providing an oscillating field empirically calibrated to 50 mV across the cell membrane. This potential difference is within physiological range, far below the thresholds of membrane electroporation (O'Neil and Tung 1991; Chen and Lee 1994) or membrane protein denaturation (Chen and Lee 1994). The initial oscillating frequency was 30 Hz, which is comparable to the natural Na/K pumping rates (Rakowski et al. 1989). After a synchronization period of 3 s (90 oscillating pulses), determined in earlier work to be sufficient to synchronize the pump molecules (Chen et al. 2007), the field frequency was gradually increased by 3% for every 10 pulses, to a final value of 400 Hz, which took about 20 s. Then, the frequency was held at 400 Hz for a period of 400–1,000 s. Fluorescence intensity was measured during the whole stimulation period, from an area on the confocal plane within the tissue slice, and plotted with time. In all experiments, the voltage-gated sodium channels were blocked using TTX so that we could focus on the field effects on the Na/K pumps.

Results

Tissue slicing is tedious, and special care and practice are needed, especially for thin slices. The unhealthy slice may

show some changes or deterioration in the preparation over the time course of the experiments. Identifying a healthy slice is important. Figure 2 is an image of a typical healthy slice, with individual myocytes observable. Striations are visible within the individual cells, and some outer cells are observed to beat during imaging. This would indicate that the cells are still alive and healthy and that the slice is viable for experimentation.

The results of measurement of TMRE fluorescence intensity presented here are averaged values. We measured the average fluorescence intensity in several regions, each containing over 100 cells. When comparing the results from a whole region with individual regions, the pattern of changes was very similar for a healthy slice, validating this averaging method. When the pattern of changes was noticeably different, the slice was considered unhealthy and abandoned.

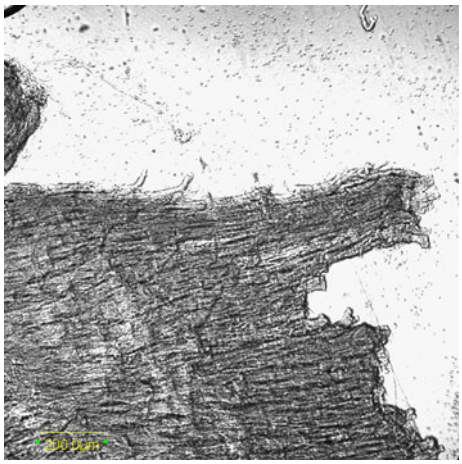

Fig. 2 Transmission image of tissue slice. Many individual cells are evident, woven into a 2-dimensional lattice

Fluorescence intensity was measured before and during the field application. In order to demonstrate the field-induced changes in the membrane potential and especially for the purpose of comparison of the results from different slices, the averaged fluorescence intensity measured before the field application functioned as a control of the slice. All results measured during the field application were normalized to this control value.

We first measured the field-induced fluorescence-intensity changes from the surface of the tissue slice. Seven tissue slices from individual rats were studied. The fluorescence changes due to the field application were averaged and plotted with standard deviation as a trace vs. the field application time, as shown in Fig. 3.

The results show that the fluorescence intensity was gradually and monotonically increased with a few seconds' time delay through the whole procedure of the field application, showing that more dye molecules penetrate the cell membrane into the cells due to the synchronization modulation electric field. Because the number of dye molecules penetrating the cell membrane into the cells depends on the membrane potential changes, this result indicates that the cell membrane potential is progressively hyperpolarized upon the field application.

At the end of the 16-min field application, the average hyperpolarization was about 9%. This value is in agreement with our earlier results taken in single skeletal muscle fibers (Chen and Dando 2007) and slightly less than that measured in single cardiomyocytes (Chen and Dando 2008). We would expect it to be more difficult to hyperpolarize the membrane potential of the aggregated cells in tissue than individual

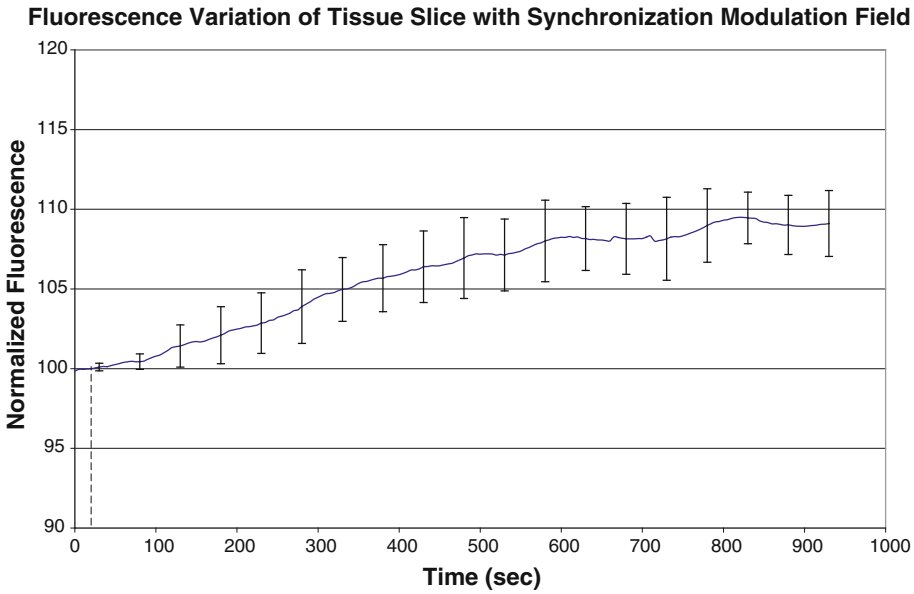

Fig. 3 Fluorescence-intensity changes measured form the surface of the tissue slice upon application of the synchronization modulation electric field, starting from the *dashed line* and lasting for about 15 min. The field frequency was initially 30 Hz and finally modulated to 400 Hz. All intensities were normalized to the value of the control measured before the field application (*dashed line*). Significant increase in fluorescence intensity within the slice is observed. Average of seven cells, with SD indicated

isolated cells. This would be due to gap junction interactions of cardiomyocytes and the difficulty in applying the electric field on individual cells due to their tight adjunction.

In the next step, we investigated the field-induced changes in the membrane potential of the interior cells in the tissue slice. Due to tight adjunction among cardiomyocytes, it may be difficult for the dye molecules to penetrate into the tissue slice. We extended our TMRE dye staining time to 30 min. Then, we measured the fluorescent intensity from the cell layers at the tissue surface and at 20 and 40 μm inside the tissues by adjusting the focus plane of the confocal microscope to the corresponding planes. The fluorescence intensities from all three cell layers were relatively consistent, though slightly lower in the deeper plane. This result implies that the dye molecules can indeed enter the slice from the surrounding reservoir solution and penetrate the cell membrane into the cells. Considering the penetration time of the dye molecules, the field application was also extended to 20 min. The field-induced changes in fluorescence intensity in three cell layers of individual slices were continuously monitored during the field application. Again, the measured fluorescence intensities were normalized to the corresponding control values measured before the field application. The results are plotted in Fig. 4.

The results show that the fluorescence intensities for all three cell layers gradually increased throughout the field application. The fluorescence intensity from the surface cell layer had the highest increment up to about 10% for 15 min field application, while the increments from the 20 and 40 μm interior cell layers were about 5% and 3%, respectively. These results indicate that the oscillating electric field can hyperpolarize the membrane potential beyond the natural resting potential even in the cell layers inside the tissue. Although there is a higher level of hyperpolarization observed at the layers proximal to the edge of the tissue slice, these are undoubtedly evidence that the oscillating electric field can penetrate into the 3-dimensional tissue matrix to hyperpolarize the membrane potential at least several cell layers into the slice.

These results were expected. Because of the voltage drop through the interstitial fluid and the tight adjunction among the cardiomyocytes in the pathway of the field application, the field-induced membrane potential on individual cells may not be the same. The deeper the cell layer is, the less the field-induced membrane potential. In addition, the series resistance in the pathway of the electric field slows down the process in charging the membrane capacitance or increases the charging time constant. Again, the deeper the cell layer is, the larger the time constant and, therefore, the more distortion of the field-induced membrane potential from the applied pulsed oscillating electric field. Our previous studies have shown that the pulsed oscillating membrane potential has the best effect in the pump synchronization, even though for those complications the results show that the synchronization modulation electric field can still noticeably hyperpolarize the membrane potential beyond the physiological value of the cell layers interior the tissue.

The above experiments were repeated seven times with different slices. A sizeable variation from slice to slice would be expected, due to differing geometry of slice arrangements, a slight variation in the direction of slicing within the heart and differing health of individual slices. However, all seven slices showed hyperpolarization of the membrane potential in interior layers upon the field application: the deeper the cell layer, the less the effect.

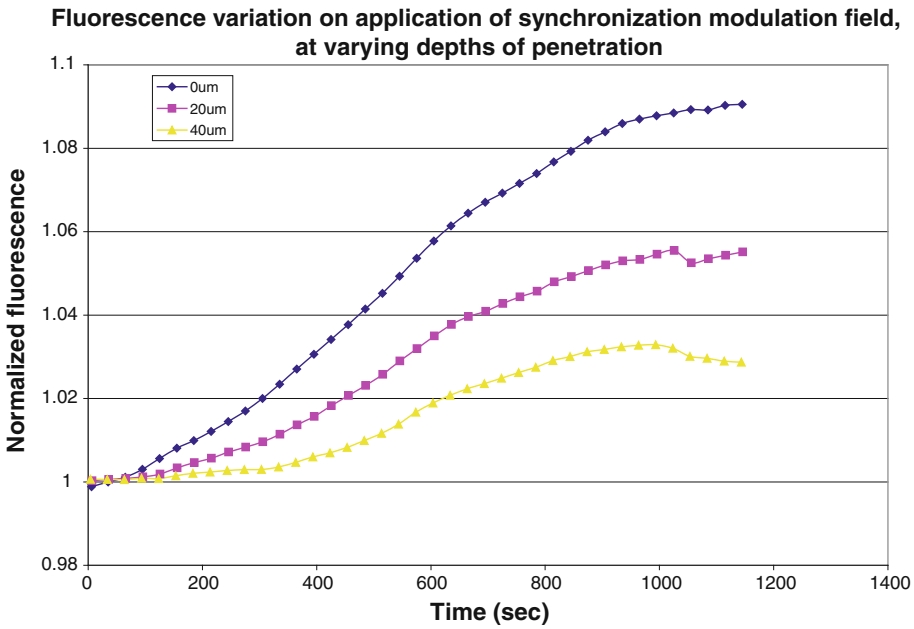

Fig. 4 Normalized fluorescence intensity vs. time of a single tissue slice, showing the relative hyperpolarization variation with different depths into the slice. Maximal effect is observed close to the surface; however, hyperpolarization is nevertheless still observed within the slice

In order to identify that the field-induced increase in the fluorescence intensity and hyperpolarization of the cell membrane were due to activation of the Na/K pump molecules, ouabain, a specific inhibitor of the Na/K pumps, was used in the following experiments. After the tissue slices were stained by the fluorescence dye, the bathing solution was changed to that with 1 mM ouabain (Sigma). Considering the penetration time of ouabain into the tissues, the oscillating electric field was not applied until 30 min later. During the field application, fluorescence intensity was monitored. Seven experiments were conducted from different tissue slices at different depths. No single slice showed an increase in fluorescence intensity upon the field application, while all seven slices exhibited some kind of decrease in intensity. The average of the seven slices is shown in Fig. 5 with standard deviation, where the dashed line represents the starting time of the field application. In 6 min of the field application, the averaged fluorescence intensity decreased over 5%. These results indicate that the field-induced membrane potential hyperpolarization is related to the Na/K pumps. Blockage of the pump functions by ouabain fully eliminated the membrane potential hyperpolarization.

In terms of the consistent decrease in the fluorescence intensity or depolarization of the membrane potential in response to the oscillating electric field, it may be due to opening of the voltage-gated potassium channels. The repeated opening in the K channels without the pump acceleration to compensate the channel currents gradually reduces the intracellular K concentration and therefore depolarizes the membrane potential.

It is also noticeable that the standard deviation of the measurements, especially to the end of the field application, is larger than that without the ouabain, as shown in Fig. 3. This may be due to the ouabain's difficulty in penetrating into the tissues to different depths of different slices. Considering that the sensitivity of the Na/K pump in cardiomyocytes to ouabain is not as high as that in skeletal muscles, we purposely used a 1 mM concentration of oubain and increased the bathing time of ouabain solution to 30 min before the field application.

Figure 6 shows the statistical distribution of tissue slice variance in response to synchronization modulation electric field in the presence and absence of ouabain. The results show that the effect of ouabain is statistically significant in response to the synchronization modulation electric field. In the control without ouabain the field-induced variance was positive and close to 10%, while in the presence of

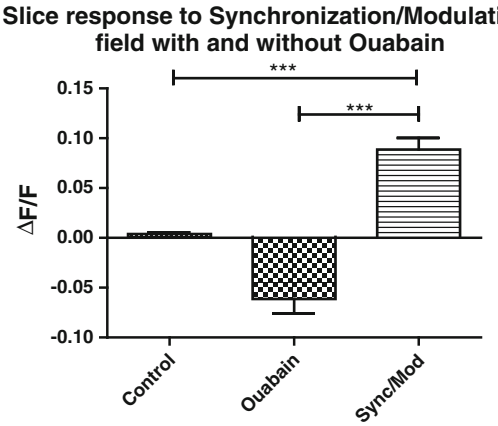

Fig. 6 Statistical distribution of tissue slice variance in response to synchronization/modulation electric field, in the presence and absence of ouabain. The results in both situations show a statistically significant response to the synchronization/modulation electric field, $***P < 0.0001$

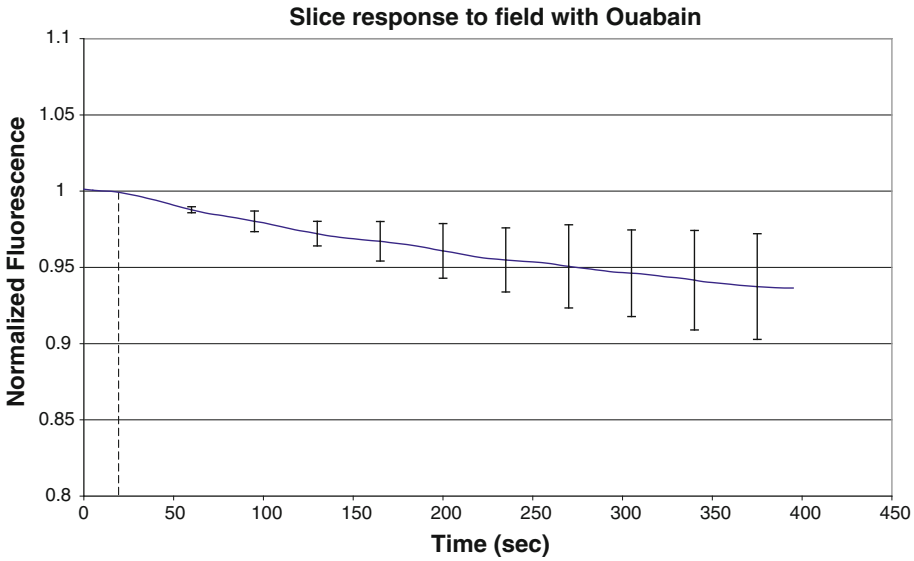

Fig. 5 Tissue slice with ouabain blocking action of Na/K-ATPase molecules, displaying normalized fluorescence intensity vs. time. Decrease in membrane potential is evident upon stimulation of slice

ouabain the variance became negative, –6%, with $P < 0.0001$. In statistical analysis carried out with GraphPad Prism (GraphPad, La Jolla, CA), P values were calculated using both repeated measures t-test for paired analysis and one-way ANOVA for unpaired analysis.

The last concern is that the field-induced hyperpolarization of the cell membrane may not be due to acceleration of the pumping rate but simply to the field application. We further conducted experiments using the backward modulation electric field, where all the field parameters and application protocol were exactly the same as forward modulation except for the modulation direction. That is, after the pump synchronization, the field oscillating frequency, instead of increasing, gradually reduced to slow down the pumping rate. Our previous studies of skeletal muscle fibers by directly monitoring the pump currents with a whole-cell patch clamp have shown that backward modulation can slow down the turnover rate of Na/K pumps.

In contrast to the use of ouabain to inhibit the pump functions, the backward modulation electric field reduces the pumping rate. This group of experiments acts as a second control whereby the tissue experiences the same magnitude of the oscillating electric field as the forward modulation. The side effect, if any, induced by the electric field on the tissue should remain the same. Any different changes in the intracellular fluorescence intensity or any alterations in the membrane potential of the tissue cells will be attributed to the method of modulation.

Similar to the forward modulation, the oscillating electric field with an initial frequency of 40 Hz and 100 oscillating pulses was first to synchronize the pump molecules. Then, the frequency gradually reduced in a stepwise pattern to 10 Hz with a step change of 3% for every 10 pulses. Once determining the minimum frequency (10 Hz), the field remained at this frequency until removal of the field.

We studied seven tissue slices from five rats. Again, no increase in fluorescence intensity was observed in all slices regardless of the depth of the cell layers upon application of the backward modulation electric field. Out of seven slices, six showed a noticeable decrease in the fluorescence intensity. The average of the seven results with standard deviation is shown in Fig. 7. The fluorescence intensity reduced about 4% in response to 6 min of backward modulation. The results indicate that the backward modulation of the oscillating electric field cannot hyperpolarize the membrane potential at all. Instead, the electric field slightly depolarized the membrane potential. This result would be again attributed to the opening of the voltage-gated potassium channels. The pump molecules with the slowed down pumping rate cannot fully compensate the channel currents and, therefore, would be unable to maintain the membrane resting potential.

From Figs. 5 and 7, it is noticed that the backward modulation shows a lesser decrease in the fluorescence intensity and therefore lesser depolarization of the membrane potential than that due to the presence of ouabain. This would make sense as in the case of ouabain the pump molecules are largely, if not entirely, inhibited from functioning and the channel currents can easily reduce the intracellular K concentration and therefore depolarize the membrane potential. Figure 5 shows the fluorescence intensity continuously reduced upon the field application. This would not be the case for the backward modulation. The pumps are still running even though significantly slowed down, which may partially compensate the channel currents. At some stage, a little over 300 s as shown in Fig. 7, the fluorescence intensity remains unchanged.

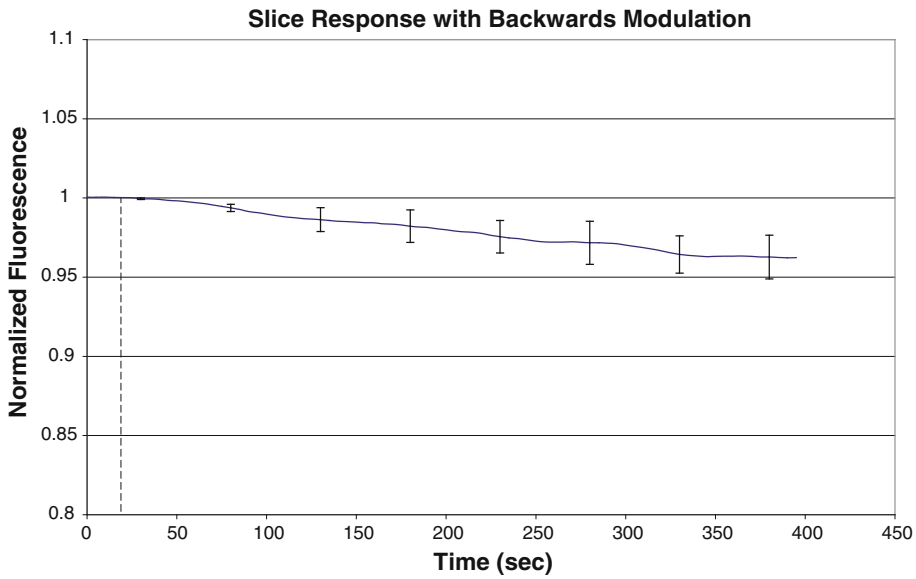

Fig. 7 Tissue slice stimulated with backward modulation, showing normalized fluorescence intensity against time. Again, slice fluorescence intensity is decreased with the stimulation

The opposite effects on the intracellular fluorescence intensity due to the two modulation electric fields, combined with the results using ouabain, provide strong evidence that the electric field alters the function of the Na/K pumps. The change of the pumping rates depends on the direction of the frequency modulation. Because all the parameters of the electric fields, as well as the protocol and configuration of the field applications, are exactly the same except for the direction of the frequency modulation, the reversal effects in the fluorescence intensity and, therefore, in the membrane potential show that the synchronization modulation electric field can effectively entrain, either accelerated or decelerated, the Na/K pumping rate.

Discussion

In this study we investigated whether the synchronization modulation electric field, which has been previously shown to effectively control the pumping rate of the Na/K pumps on single isolated cells, can manipulate the membrane potential in a 3-dimensional tissue slice.

When applying an oscillating electric field to aggregated cells in 3-dimensional tissues to activate the Na/K pump functions, we have to consider two things. One is the possible side effects of the applied electric field on other membrane proteins, especially the voltage-dependent membrane proteins. Another is how the applied electric field generates the necessary oscillating membrane potential for both magnitude and waveform in individual cells of the tissues and effectively activates the pumps in the presence of cell-to-cell interaction and regulatory mechanisms.

In terms of side effects, the major voltage-dependent membrane proteins in cardiac muscle cells are the voltage-gated Na channels, delayed rectifier K channels, inward rectifier K channel and L-type Ca channels. Our previous voltage-clamp studies have shown that an oscillating membrane potential can effectively inactivate the delayed rectifier K channel. The rectifier K channel currents can be significantly reduced even within the synchronization period (not published). In this study, the voltage-gated Na channels were blocked by TTX. In fact, the inactivation of the Na channel is well known and more obvious than that in the K channel. In terms of inward rectifier K channels, indeed, we did not specifically study their inactivation. However, the inward rectifier K channel opens when the membrane potential is hyperpolarized, resulting in K ion influx. If the oscillating electric field cannot inactivate the inward rectifier K channels, the channel opening and the resultant K ion influx will hyperpolarize the membrane potential, which is consistent with the effects of Na/K pump activation. For other membrane proteins, such as the L-type Ca channels, even if they cannot be inactivated, the ion flux is much smaller than in the Na and K channels; and these will not affect the membrane potential significantly.

In fact, our previous studies have shown that the synchronization modulation electric field can hyperpolarize membrane potential of single skeletal muscle fibers in physiological solution without any channel blockers (Chen and Dando 2007). We observed that upon the field application, the membrane potential was initially and quickly depolarized for a short period due to opening of Na channels and then gradually hyperpolarized until removal of the field. Here, we show the field-induced slow hyperpolarization of the membrane potential without transient initial depolarization, which is consistent with our previous studies.

In terms of the difficulty in alternating the membrane potential in individual cells of 3-dimensional tissue and the cell-to-cell interaction, the results clearly show that the electric field can effectively increase the fluorescence intensity and, therefore, the hyperpolarizing membrane potential of the cells persisted to a level of several cell layers into the slice. Indeed, the deeper into the tissues, the less hyperpolarization of the membrane potential was observed.

The fact that the hyperpolarizing effect was eliminated when either the Na/K pumps are chemically blocked with ouabain or the modulation is performed backward would suggest not only that are the effects attributable to the activation on the Na/K pumps but also that the pump molecules can be entrained oppositely. This, in turn, would suggest that we are exhibiting a degree of control over the action of these critical physiological housekeeping molecules at the tissue level, which would provide promise for the future application of the technique.

The transposing of the field application on single cells to cell aggregation in the tissue matrix has a great deal of promise. The contribution of interactions between neighboring cells in the matrix (i.e., connexons) was found to be trivial in front of active entrainment of the pump molecules, with the cell membrane hyperpolarization at a rate and to a level approximated to the behavior observed from single isolated cells.

The success from single cells to tissue slices without much detriment to the level of measured effectiveness suggests that the next logical step would be to apply the technique to a large tissue sample or even a small organ.

Acknowledgement This study was partially supported by research grants from the National Institutes of Health (GM R01 50785) and National Science Foundation (0515787).

References

Albers RW (1967) Biochemical aspects of active transport. Annu Rev Biochem 36:727–756

Astumian RD (1997) Thermodynamics and kinetics of a brownian motor. Science 276:917

Astumian RD (2003) Adiabatic pumping mechanism for ion motive ATPases. Phys Rev Lett 91(11):118102

Blank M, Soo L (1989) The effects of alternating current on Na, K ATPase function. Bioelectrochem Bioenerg 22:313–322

Chen W (2008) Synchronization of ion exchangers by an oscillating electric field: theory. J Phys Chem B 112(32):10064–10070

Chen W, Dando R (2007) Electrical activation of Na/K pumps can increase ionic concentration gradient and membrane resting potential. J Membr Biol 39:117–126

Chen W, Dando R (2008) Membrane potential hyperpolarization in mammalian cardiac cells by synchronization modulation of Na/K Pumps. J Membr Biol 221(3):165–173

Chen W, Huang F (2008) Computer simulation of synchronization of Na/K pump molecules. J Bioenerg Biomembr 40:337–345

Chen W, Lee RC (1994) An improved double vaseline gap voltage clamp to study electroporated skeletal muscle fibers. Biophys J 66:700–709

Chen W, Zhang ZS, Huang F (2007) Entrainment of Na/K pumps by synchronization modulation electric field. J Bioenerg Biomembr 39:331–339

Chen W, Zhang ZS, Huang F (2008) Synchronization of the Na/K pumps by an oscillating electric field. J Bioenerg Biomembr 40:347–357

Conway MJ, Seibel JA, Eaton RP (1974) Thyrotoxicosis and periodic paralysis: improvement with beta blockade. Ann Intern Med 81:332–336

De Paoli F, Overgaard K, Nielsen OB (2002) Protective effects of acidosis and Na/K pump activation on force in K depressed skeletal muscle. J Physiol (Lond) 544:82P

Desnuelle C, Lombet A, Serratrice G, Lazdunski M (1982) Sodium channel and sodium pump in normal and pathological muscles from patients with myotonic muscular dystrophy and lower motor neuron impairment. J Clin Invest 69:358–367

Everts ME, Skajaa K, Hansen K (1990) The concentration of ouabain biding sites in biopsies of uterine muscle. Acta Physiol Scand 139:503–510

Evertsen F, Medlbo JI, Jebens E, Nicolaysen K (1997) Hard training for 5 mo increases Na/K pump concentration in skeletal muscle of cross-country skiers. Am J Physiol Regul Integr Comp Physiol 272:R1417–R1424

Haller RG, Clausen T, Vissing J (1998) Reduced levels of skeletal muscle Na^+, K^+-ATPase in McArdle disease. Neurology 50: 37–40

Huang F, Rabson D, Chen W (2009) Distribution of the Na/K pumps' turnover rates as a function of membrane potential, temperature, and ion concentration gradients and effect of fluctuations. J Phys Chem B 113(23):8096–8102

Lee RC, Kolodncy MS (1987) Electrical injury mechanisms: dynamics of the thermal response. Plast Surg 80:663

Lee RC, Gaylor DG, Bhatt DL, Israel DA (1988) Role of cell membrane rupture in the pathogenesis of electrical trauma. J Surg Res 44(6):709

Loew LM (1993) Confocal microscopy of potentiometric fluorescent dyes. Methods Cell Biol 38:195–209

O'Neil RJ, Tung L (1991) Cell-attached patch clamp study of the electropermeabilization of amphibian cardiac cells. Biophys J 59:1028–1039

Phipps J, Yee P, Fletcher E, Vingrys A (2006) Rod photoreceptor dysfunction in diabetes: activation, deactivation, and dark adaptation. Invest Ophthalmol Vis Sci 47(7):3187–3194

Post RL, Jolly PC (1957) The linkage of sodium, potassium and ammonium active transport across the human erythrocyte membrane. Biochim Biophys Acta 25:118–128

Rakowski RF, Gadsby DC, De Weer P (1989) Stoichiometry and voltage dependence of the sodium pump in voltage-champed, internally dialyzed squid giant axon. J Gen Physiol 93:903–941

Scherzer P, Nachlie I, Bar-On H, Popovtzer M, Ziv E (2000) Renal Na/K ATPase hyperactivity in diabetic psammomys obesus is related to glomerular filtration but is insulin-independent. J Endocrinol 167:347–354

Serpersu EH, Tsong TY (1983) Stimulation of a ouabain-sensitive Rb^+ uptake in human erthrocytes with an external electric field. J Membr Biol 74:191–201

Sima AA, Zhang W, Li ZG, Murakawa Y, Pierson CR (2004) Molecular alterations underlie nodal and paranodal degeneration in type 1 diabetic neuropathy and are prevented by C-peptide. Diabetes 53:1556–1563

Skou J (1957) The influence of some cations on an adenosine triphosphatase from peripheral nerves. Biochim Biophys Acta 23(2):394–401

Stevens MJ, Lattimer SA, Kamijo M, Van Huysen C, Sima AA, Greene DA (1993) Osmotically-induced nerve taurine depletion and the compatible osmolyte hypothesis in experimental diabetic neuropathy in the rat. Diabetologia 36:608–614

Teissie J, Tsong TY (1980) Evidence of voltage-induced channel opening in Na/K ATPase of human erythrocyte membrane. J Membr Biol 55:133–140

Tsien RY, Waggoner AS (1990) Fluorophors for confocal microcopy. In Handbook of confocal microscopy. Plenum Press, New York, pp 169–178

Tsong TY (2002) Na, K-ATPase as a brownian motor: electric field-induced conformational fluctuation leads to uphill pumping of cation in the absence of ATP. J Biol Phys 28(2):309–325

Tsong TY, Astumian RD (1987) Electroconformational coupling and membrane protein function. Prog Biophys Mol Biol 50:1–45

Waggoner AS (1976) Optical probes of membrane potential. J Membr Biol 27(4):317–334

Wahren J, Ekberg K, Johansson J, Henriksson M, Pramanik A, Johansson BL (2000) Role of C-peptide in human physiology. Am J Physiol Endocrinol Metab 278:E759–E768

Weaver JC, Astumian RD (1990) The response of living cells to very weak electric fields: the thermal noise limit. Science 247:459

Xie TD, Marxzalek P, Chen YD, Tsong TY (1994) Recognition and processing of randomly fluctuating electric signals by Na, K-ATPase. Biophys J 67:1247–1251

Yuk-Chow NG, Tolerico PH, Book CBS (1993) Alternations in levels of Na/K ATPase isoforms in heart, skeletal muscle, and kidney of diabetic rats. Am J Physiol Endocrinol Metab 265:E243–E251